QUINOL-CYTOCHROME *C* OXIDOREDUCTASE AND CYTOCHROME C_4 MEDIATE ELECTRON TRANSFER DURING SELENATE RESPIRATION IN *THAUERA SELENATIS**

Elisabeth C. Lowe[1], Sarah Bydder[2], Robert S. Hartshorne[3], Hannah L.U. Tape[1], Elizabeth J. Dridge[1], Charles M. Debieux[1], Konrad Paszkiewicz[1], Ian Singleton[4], Richard J. Lewis[5], Joanne M. Santini[6], David J. Richardson[3] and Clive S. Butler[1]

[1]School of Biosciences, Centre for Biocatalysis, University of Exeter, Stocker Road, Exeter EX4 4QD, UK
[2]Department of Microbiology, La Trobe University, 3086 Victoria, Australia
[3]School of Biological Sciences, University of East Anglia, Norwich NR4 7TJ, UK
[4]Institute for Research on Environment and Sustainability, University of Newcastle, Newcastle upon Tyne NE2 4HH, UK
[5]Institute for Cell and Molecular Biosciences, University of Newcastle, Newcastle upon Tyne NE2 4HH, UK
[6]Institute of Structural and Molecular Biology, UCL, Gower Street, London WC1E 6BT, UK

Running head: Pathways of electron transfer in *T. selenatis*

Address correspondence to: Clive S. Butler, School of Biosciences, Centre for Biocatalysis, University of Exeter, Stocker Road, Exeter, UK. EX4 4QD. Fax: +44 1392 263434; E-mail: c.s.butler@exeter.ac.uk

Selenate reductase (SER) from *Thauera selenatis* is a periplasmic enzyme that has been classified as a type II molybdoenzyme. The enzyme comprises three subunits SerABC, where SerC is an unusual *b*-heme cytochrome. In the present work the spectropotentiometric characterization of the SerC component and the identification of redox partners to SER are reported. The mid-point redox potential of the *b*-heme was determined by optical titration (E_m +234±10 mV). A profile of periplasmic *c*-type cytochromes expressed in *T. selenatis* under selenate respiring conditions was undertaken. Two *c*-type cytochromes were purified, (~24 kDa and ~6 kDa), and the 24 kDa protein (cyt*c*-Ts4) was shown to donate electrons to SerABC *in vitro*. Protein sequence of cyt*c*-Ts4 was obtained by N-terminal sequencing and LC-MS/MS analysis, and based upon sequence similarities, was assigned as a member of cytochrome c_4 family. Redox potentiometry, combined with UV-visible spectroscopy, showed that cyt*c*-Ts4 is a diheme cytochrome with a redox potential of +282±10 mV and both hemes are predicted to have His-Met ligation. To identify the membrane-bound electron donors to cyt*c*-Ts4, growth of *T. selenatis* in the presence of respiratory inhibitors was monitored. The specific quinol-cytochrome *c* oxidoreductase (QCR) inhibitors myxothiazol and antimycin A partially inhibited selenate respiration, demonstrating that some electron flux is *via* the QCR. Complete inhibition of selenate respiration was achieved with the more general inhibitor 2-n- heptyl- 4-hydroxyquinoline N-oxide (HQNO). Electron transfer *via* a QCR and a diheme cytochrome c_4 is a novel route for a member of the DMSO reductase family of molybdoenzymes.

Within the DMSOR[1] family of type II molybdoenzymes (1) there is a distinct clade of enzymes that are translocated to the periplasm using the twin arginine translocation (TAT) pathway (2,3) and possess a monomeric *b*-type heme-containing γ-subunit (1). The enzymes within this clade function as either dehydrogenases (e.g. ethylbenzene dehydrogenase from *Aromatoleum aromaticum* (4), dimethylsulphide dehydrogenase from *Rhodovulum sulfidophilum* (1,5) or reductases (e.g. selenate reductase from *Thauera selenatis* (6,7), chlorate reductase from *Ideonella dechloratans* (8,9), and catalyze either hydride or oxygen transfer as generalized by equation [1].

$$X + H_2O \leftrightarrows XO + 2H^+ + 2e^- \qquad [1]$$

These soluble enzymes consist of three subunits and in addition to the *b*-heme cytochrome (γ-subunit), they comprise an iron-sulfur protein (β-subunit) co-ordinating 1x[3Fe-4S] cluster and 3x[4Fe-4S] clusters, and a catalytic component (α-subunit) that co-ordinates a [4Fe-4S] cluster and the active site molybdenum

[1] MGD, molybdenum guanine dinucleotide; SER, periplasmic selenate reductase; NAR, membrane-bound nitrate reductase; EBDH, ethylbenzene dehydrogenase; DMSDH, dimethyl sulfide dehydrogenase; DMSOR, dimethylsulfoxide reductase; FDH, formate dehydrogenase; FeS/FS0, iron-sulfur clusters; HQNO, 2-n-heptyl-4-hydroxyquinoline N-oxide; TMAOR, trimethylamine N-oxide reductase; TAT, twin-arginine translocation; QCR, quinol-cytochrome *c* oxidoreductase; QDH, quinol dehydrogenase; DH, primary dehydrogenase; PMF, proton-motive force; OFN, oxygen free nitrogen.

guanine dinucleotide (MGD) cofactor (10,11) (Figure 1). The reductases play a pivotal function, coupling the reduction of substrates to the generation of the proton motive force (PMF). Identifying the route by which electrons are transferred to these reductases is vital to understanding their bioenergetics (12). How periplasmic substrate reduction can generate a PMF, that is sufficient to support growth, is of considerable interest. The use of selenate and selenite as bacterial respiratory substrates has been well documented (13). By far the most well studied selenate-respiring bacterium has been *T. selenatis*; however, the characterisation of the selenate respiratory system has not yet addressed the mechanism by which electrons are transferred from the cytoplasmic membrane to the periplasmic selenate reductase (SerABC). As SerABC appears to be soluble and not associated with the inner or outer membrane (6), it is likely that another protein acts as a shuttle to take electrons from the membrane and deliver them to the *b*-heme of SerC. Reduced SerC then donates electrons, *via* the iron-sulfur clusters of SerAB (11), specifically to the molybdopterin co-factor for reduction of selenate (SeO_4^{2-}) to selenite (SeO_3^{2-}) (6,14,11).

The *b*-heme of SerC is presumed to be the site of electron entry to the SER enzyme complex, but also remains poorly studied. The recently solved crystal structure of ethylbenzene dehydrogenase (EBDH) reveals that its γ-subunit also binds an unusual *b*-type heme, which is coordinated by methionine and lysine ligands (15). This co-ordination favours the uncharged ferrous heme over the charged ferric form and as such modulates a relatively high redox potential of +254 mV. Similarly, optical potentiometeric redox titrations of the heme *b* in the γ-subunit of dimethylsulphide dehydrogenase (DMSDH) revealed a high redox potential of E_m = +324mV (10). By contrast, the cytoplasmic-facing respiratory nitrate reductase NAR from *Escherichia coli* (another member of the type II molybdoenzymes) possesses a membrane bound γ-subunit (NarI) that co-ordinates two *bis*-His ligated *b*-hemes that have much lower redox potentials at +20 and +120 mV (16). In the case of NAR, the low redox potentials of the heme favours electron flow away from NarI, towards the MGD cofactor in NarG, and ultimately resulting in the reduction of nitrate to nitrite. Critically, the dehydrogenases (EBDH and DMSDH) function in the reverse direction (figure 1); it has been argued that due to the unusually high potential *b*-heme in γ-subunits of both EBDH and DMSDH, that the γ-subunit is the site of electron egress from these enzymes to their redox partners (10,15). Consequently, the high potential *b*-heme might function to draw electrons away from, rather than towards, the MGD cofactor during catalysis as displayed in the nitrate reductase enzymes. Analysis of the amino acid sequence alignment of EBDH and DMSDH with selenate reductase (SER) shows that the co-ordinating methionine (M138) and lysine (K228) residues are also conserved in SerC. This then raises interesting questions as to what is the redox potential for the *b*-heme in the reductase members of this distinct type II clade and what are the likely redox partners?

Among the related type II molybdoenzymes, there are a number of different routes of electron transfer to terminal reductases, although the majority catalyze reactions with a lower redox potential than the selenate/selenite couple (+475 mV). For example; the DMSO/DMS couple is +160 mV and TMAO/TMA couple is +130 mV (17). Within the DMSOR group, a number of pathways for electron transport have been established, and a variety of membrane-bound proteins have been implicated. These membrane-bound cytochromes are responsible for extracting electrons from the quinol pool so that they can be transferred to the associated downstream terminal reductases. The existing literature provides several routes by which electrons are transferred. For example, the membrane bound nitrate reductase NarGH (16,18) receives its electrons from its dedicated NarI membrane integral subunit, which contains two *b*-hemes; the DMSO reductase from *E. coli* (DmsABC) has a similar organisation of subunits (17), but faces the periplasm. The *E. coli* TMAO reductase TorA (*Rhodobacter* sp.), DMSO reductase DorA (17), and the periplasmic nitrate reductase NapAB (19) accept electrons from dedicated tetra or penta-heme quinol dehydrogenases in the membrane (TorC/DorC/NapC). In the case of Nap, there is also an alternative pathway; the *nap* gene cluster in *E. coli* for example, also contains *napG* and *napH*, which encode iron-sulfur proteins responsible for electron transfer from ubiquinol to NapC (20).

It may be the case that selenate respiration in *T. selenatis* does not occur *via* any of these known pathways; McEwan *et al*. (21) postulated that the selenate reductase of *T. selenatis* could receive electrons from quinol-cytochrome *c* oxidoreductase (QCR) *via* a high-potential *c*-type

cytochrome, due to the high potential of the selenate/selenite couple. This has not been seen for any of the other type II molybdoenzymes so showing electron donation from QCR, *via* a soluble cytochrome *c* to SerABC would represent a novel electron transport chain within this group. The aim of the present work was to resolve the electron transfer pathways during selenate respiration in *T. selenatis*.

EXPERIMENTAL PROCEDURES

Growth of T. selenatis, production of periplasmic fractions and purification of SER. - *T. selenatis* was grown anaerobically at 30°C in mineral salts medium (6) containing yeast extract (0.1%), with either selenate or nitrite (10 mM) as terminal electron acceptors and acetate (10 mM) as the electron donor in 10 L batch cultures. Cultures were harvested during late log phase (after 16-18 hours growth) at A_{600} 0.6-0.7 and spheroplasts were prepared as described previously (6). The spheroplasts were removed by centrifugation (25,000 x *g*, 20 minutes) and the supernatant, containing the periplasm, was retained. Periplasms were analysed by SDS-PAGE and *c*-type cytochromes were visualised using the heme stain method. SER was purified as detailed by Schröder *et al*. (6) with the modifications noted by Dridge *et al*. (11). Purified enzyme was stored at -80°C. Purity was determined by SDS-PAGE and positive identification of the presence of the SerC component was achieved by N-terminal sequence analysis as described previously (22).

Purification of c-type cytochromes - Soluble protein from a 10 L culture, was loaded onto a Q-Sepharose Fast-Flow anion exchange column (70 ml bed volume) (GE Healthcare) pre-equilibrated with 3 column volumes of 30 mM Tris, pH 8.5. The column was washed with a further column volume of buffer to remove unbound proteins. A 24 kDa *c*-type cytochrome was eluted using a 300 ml gradient of 0-300 mM NaCl in 30 mM Tris, pH 8.5. Protein concentration was monitored using absorbance at 280 nm and presence of cytochromes was monitored using absorbance at 410 nm. The fractions containing the 24kDa *c*-type cytochrome as determined by SDS-PAGE were pooled and concentrated using a 15 ml 10 kDa MWCO centrifugal concentrator at 4000 x *g*. The concentrated protein was loaded onto a Superdex 200 16/60 gel filtration column (GE Healthcare) equilibrated with 2 column volumes of 30 mM Tris, pH 8.5 and eluted in the same buffer. The fractions containing the 24kDa *c*-type cytochrome were pooled and loaded onto a 1 ml MonoQ anion exchange column (GE Healthcare) equilibrated with 30 mM Tris, pH 8.5 and eluted with a gradient of 0-1 M NaCl in 30 mM Tris, pH 8.5. As a final purification step, the fractions containing the 24 kDa *c*-type cytochrome were pooled and transferred to dialysis tubing (6 kDa MWCO) (Fisher), the protein was then dialysed overnight at 4°C, with gentle stirring, into 30 mM Tris, pH 8.5, containing 1 M ammonium sulfate. The dialysed protein was bound to a 25 ml Fast-Flow Phenyl Sepharose column (GE Healthcare) pre-equilibrated with 1 M ammonium sulfate in 30 mM Tris, pH 8.5, and subsequently eluted with a decreasing gradient of 1 to 0 M ammonium sulfate. The cytochrome was judged pure by SDS-PAGE, concentrated as before and stored at 4°C for short term use, or -80°C for longer term storage. All chromatography procedures were carried out using an AKTAPrime (GE Healthcare) purification system, except for the MonoQ column which was run on an AKTABasic (GE Healthcare). The soluble fraction from a 2 L culture was also prepared as described above. This soluble fraction was concentrated using a 15 ml 5 kDa MWCO centrifugal concentrator (Millipore) to a final volume of 5 ml, and then loaded onto a Superdex 200 16/60 gel filtration column pre-equilibrated with 20 mM Tris, pH 8.0. Proteins were eluted in the same buffer. Fractions were monitored for presence of protein using the absorbance at 280 nm for presence of cytochrome using the absorbance at 410 nm. Fractions containing the 6 kDa cytochrome were identified by SDS-PAGE, pooled, and concentrated in a 5 ml 5 kDa MWCO concentrator.

Electronic absorption spectroscopy - UV-visible spectra of protein samples were recorded on a Varian Cary 4E UV/Vis spectrophotometer between 350-650 nm. Reduced samples were achieved by adding excess sodium dithionite and oxidized samples by the addition of potassium ferricyanide.

Electron transfer assay - To determine whether purified cytochromes were able to donate electrons to SerABC *in vitro*, a solution of approximately 5 µM cytochrome in 50 mM phosphate buffer (pH 7.5) was degassed in a sealed cuvette. A weak solution (10 mM) of sodium dithionite was also degassed and then titrated into the cuvette using a 10 µl Hamilton

syringe, until the cytochrome was fully reduced, as determined by wavelength scanning UV-visible spectroscopy (350-700 nm). SerABC and selenate were added to final concentrations of 1 µM and 20 mM respectively, and re-oxidation of the cytochrome monitored by recording the spectra. Cytochromes were similarly tested for selenate and selenite reductase activity by incubation with the relevant substrate but no SerABC.

Optical redox titrations - Optical spectra of the samples were measured on a Hitachi U-3310 spectrophotometer between 350-700 nm. Protein samples were added to a stirred cuvette constantly sparged with OFN to minimise oxidation from air. Redox mediators (2,3,5,6 tetramethyl-p-phenylendiamine, 1,2 napthoquinone, phenozinemethosulfate, phenylethosulfate, juglone, duroquinone, menadion) were added to a final concentration of 6 µM each, and the potential measured using an electrode (23). The electrode was initially calibrated with reference to a saturated solution of quinhydrone (295 mV vs. SHE). A degassed solution of 5 mM sodium dithionite was prepared and added in 1 µl steps, recording the potential, and the spectra at each step. Once the sample was fully reduced, 3 mM potassium ferricyanide was titrated in similarly to re-oxidise the sample. The fraction of protein reduced at each potential was calculated and fitted to a Nernstian equation using the curve fitting program TableCurve 2D (Systat Software Inc.).

Sequence analysis of the 24 kDa cytochrome - N-terminal sequencing of the 24 kDa cytochrome was undertaken at the Pinnacle Proteomic facility, Newcastle University. Native 24 kDa cytochrome *c* was also digested in solution using Trypsin Gold (Promega) according to the manufacturers' instructions. Briefly, Trypsin Gold in 50 mM acetic acid was mixed with the cytochrome (in 30 mM Tris, pH 8.5) in a ratio of 1:20 w/w protease:protein. The mixture was incubated at 37°C for 1 hour, and analysed by SDS-PAGE. Protein bands of interest were excised for analysis, which was carried out using LC-MS/MS at the University of York Proteomics department.

Sequencing the T. selenatis genome using Illumina sequencing - Genomic DNA was extracted and fragmented to using the Bioruptor apparatus and fragments of 200 bp were selected using an agarose gel purification protocol. These fragments were then prepared using the standard Illumina paired-end library preparation protocols. The resulting DNA was purified using an acrylamide gel and these were sequenced using an Illumina GA2 sequencer using a single lane loaded at 6pM. Illumina version 2 reagents were used together with Illumina SCS 2.3 and Illumina Pipeline 1.3 software to base call. This produced 15,422,089 36bp paired-end sequences. These were subsequently trimmed to remove or shorten reads which contained adaptor sequence. Read 2 contained unusually high error rates toward the 3' end of the reads. Where appropriate these were shortened prior to any de-novo assembly to remove bases with quality scores less than 20.

MAQ (http://maq.sourceforge.net/) was used to align these sequences to the reference genome *Thauera MZ1T (Genbank accession CP001281 and CP001282).* This was achieved with an average depth of 32.9 across non-gap regions. Unmapped reads were then collated and assembled de-novo using Velvet (version 0.7.47) in single-end mode using a hash length of 21 (24). These unmapped reads generated an assembly with 14,870 contigs and an N50 length of 1223 bp. These contigs represent genomic regions present in *T. selenatis* but which are absent in *Thauera MZ1T*. Additionally a completely *de-novo* assembly was produced using Velvet in paired end mode using a parameter sweep of hash length and coverage cut-off. A hash length of 25 and a coverage cut-off of 5 was found to produce the highest N50. This resulted in an assembly of 769 contigs with an N50 value of 135, 919 bp (made up of 17 contigs) and a total length of 9.48Mb.

Micro-culture growth and respiratory inhibition studies - In order to monitor the effects of changing culture conditions and inhibitors on the growth of *T. selenatis*, a method utilising micro-culture was developed. A 500 ml bottle of mineral salts medium was prepared without the addition of selenate or other electron acceptor. The bottle was sealed with rubber septa and sparged with OFN for at least 1 hour. Each well of a 96-well microtitre plate had 250 µl of the degassed medium added to it, and electron acceptor added in varying concentrations from degassed stock solutions. Inhibitors, myxothiazol, antimycin A and HQNO, at a range of concentrations, were added to wells as required. Wells were inoculated with 1 µl washed cells from an exponential phase *T. selenatis* culture (1 ml of cells at OD_{600nm} 0.6-0.7 were harvested by centrifugation at 12,000 x *g*, 2 minutes, and resuspended in 1 ml of the degassed media).

Inoculated plates were incubated in a FLUOstar Optima microplate reader (BMG Labtech) attached to a nitrogen cylinder to keep the plate in an anaerobic atmosphere. The plate was maintained at a constant temperature of 30°C, and OD_{600nm} values were measured in each well every 15 minutes using the kinetics measuring program, with 5 seconds shaking before each reading. Each plate had 6 wells without the addition of bacteria to ensure no contaminants were growing, and to act as a baseline, and 6 wells with non-inhibiting growing conditions for *T. selenatis* to check the culture was growing typically. The maximum gradient at exponential growth was determined by fitting the growth curves to the Gompertz equation (25). All growth conditions were replicated at a range of substrate concentrations and using non-linear regression, the maximum growth rate (μ_{max}) of the culture was calculated using the Monod equation [2] (26):

$$\mu = \mu_{max} ([S]/K_s + [S]) \quad [2]$$

RESULTS

Cytochrome c profile during selenate respiration - The *c*-type cytochromes expressed during selenate respiration in *T. selenatis* were profiled by heme staining SDS-PAGE resolved periplasmic proteins. Several soluble cytochromes were identified (referred to as cyt*c*-Ts1-Ts7; in size order) (Figure 2A) and by comparing the expression profile to nitrate grown cells, a number of cytochromes were found to be more highly expressed during selenate respiration. Cyt*c*-Ts1 is present under both growth conditions but to a lesser extent when grown on selenate. Cyt*c*-Ts2 is poorly resolved but present as a band at approximately 40 kDa in selenate grown cells. Cyt*c*-Ts3 (~33 kDa) is again expressed under both growth conditions. Cytochromes identified as cyt*c*-Ts5 and cyt*c*-Ts6 were resolved only in selenate grown cells. Cyt*c*-Ts4 (24 kDa) and cyt*c*-Ts7 (6 kDa) were both significantly up-regulated under selenate growth conditions and selected for further investigation. Cyt*c*-Ts4 and cyt*c*-Ts7 were purified (Figure 2A) and tested as potential electron donors to SerABC.

Characterisation of 6 kDa cytochrome (cytc-Ts7) - The reduced UV-visible spectrum of the purified 6 kDa cytochrome (cyt*c*-Ts7) was typical of a low-spin *c*-type cytochrome, with absorbance maxima at 415, 522 and 551 nm (Figure 2C). The oxidized spectrum shows a shift in the Soret band to 409 nm and a broad feature around 525 nm. In order to test the ability of this cytochrome to donate electrons to SerABC, it was reduced by titration with a weak solution of sodium dithionite, and mixed with purified selenate reductase and selenate in an anaerobic assay. No re-oxidation of the heme was observed suggesting that the 6 kDa cytochrome is not able to act as electron donor to SerABC *in vitro* (data not shown).

Characterisation of the 24 kDa cytochrome (cytc-Ts4) - UV-visible spectroscopy of the 24 kDa cytochrome (cyt*c*-Ts4) is again typical of a low-spin heme *c* (Figure 2B). It is purified in a partially reduced state, but does not readily become oxidized, even after lengthy exposure to air. Protein reduced with dithionite shows a Soret band at 414 nm, an α-band at 550 nm and a β-band at 519 nm. The α-band shows asymmetry, with a shoulder at 545 nm suggesting a composite band, possibly due to the presence of more than one heme in the protein. Oxidized with ferricyanide, the cytochrome has a Soret band at 409 nm and a broad feature at 528 nm. As for cyt*c*-Ts7, cyt*c*-Ts4 was tested for its ability to donate electrons to SerABC in an anaerobic assay. In this case, after incubation with enzyme and substrate, the visible absorbance spectrum is shifted (Figure 3). The Soret band shifts from 414 nm to 410, and decreases in intensity, and the α/β peaks broaden and decrease in intensity, indicative of re-oxidation of the heme. Cyt*c*-Ts4 incubated with SerABC, selenate or selenite alone did not exhibit any shifts in absorbance (data not shown), suggesting that this cytochrome is capable of donating electrons to SerABC for the reduction of selenate to selenite *in vitro*, and therefore could be an *in vivo* electron donor to SerABC. The rate of cyt*c*-Ts4 heme oxidation was determined to be some 50 times slower than the observed rate of SER turnover determined using methyl viologen as the electron donor (6). Similarly, Craske and Ferguson (27) have shown that NAR from *P. denirificans* has a 50-fold higher V_{max} with methyl viologen than with duroquinol.

Determination of the redox potential of cytc-Ts4 - The redox potential of the heme of cyt*c*-Ts4 was measured spectrophotometrically by monitoring the absorbance of the α-band at 551 nm (adjusted by reference to an isosbestic point at 560 nm) during reduction or oxidation of the heme (Figure 4A). The fraction of protein reduced

at each measured potential was calculated, then plotted as a function of redox potential vs. the standard hydrogen electrode (SHE) (Figure 4B). Nernst curves for n=1 and n=2 (where n is number of electrons transferred) were fitted and are also shown in figure 4B. Interestingly, the data fits more closely to an n=2 curve, suggesting the cytochrome has 2 hemes. A mid-point potential of +282 ±10 mV for the cytochrome was calculated, but we were unable to resolve 2 separate potentials.

Sequence determination and analysis - MALDI-TOF analysis of cyt*c*-Ts4 gave a molecular weight of 23,558 Da, not including heme groups. N-terminal sequencing (Pinnacle Proteomic facility, Newcastle University) and LC-MS/MS of tryptic digest fragments (University of York Proteomics dept.) resulted in 60 aa of sequence data which was used to identify the gene for this cytochrome from the draft genome assembly of *T. selenatis*. Peptides were searched against a custom Blast (28) database containing all contigs generated from the sequence data which could not be mapped to *Thauera MZ1T* and separately to another database containing the complete set of contigs generated from all Illumina *T.selenatis* data. Due to the short lengths of the peptides only 2 significant hits were obtained and these contigs were used as targets for further investigation. ORF prediction was carried out using the CLC-Bio software package and candidate regions searched *via* Blast against the non-redundant database of protein sequences. The sequence of cyt*c*-Ts4 (*Genbank accession* GU570563) was used to search the database and an alignment of similar cytochromes is shown in supplemental figure S1. Alignment of the predicted amino acid sequences shows the presence of two conserved CXXCH motifs consistent with the binding of two covalently attached hemes. The presence of two further conserved methionine residues suggests that both hemes are His-Met co-ordinated.

Determination of the redox potential of the b-heme in SerC - Purified SER was used to determine the midpoint potential of the *b*-heme in SerC, the point of electron entry to the reductase from the cyt*c* redox partner. The redox potential of the heme was determined by optical redox titration by monitoring the absorbance of the heme at 558 nm (adjusted with reference to an isosbestic point at 575 nm) during sequential oxidation and reduction of the heme (Figure 5A). The slight drift observed in the spectrum is due to the contribution of the [Fe-S] clusters in SerAB. The absorbance was monitored at the α-band wavelength rather than that of the Soret band, as the redox mediators used do not absorb in the α-band region, but might interfere at Soret band wavelengths. The fraction of protein reduced at each measured potential was calculated and then plotted as a function of redox potential (Figure 5B). The Nernst curve corresponding to n=1 electrons was fitted to the data giving a midpoint potential of +234±10 mV.

Quinol-cytochrome c oxidoreductase is an electron donor to selenate reductase in T. selenatis - Soluble cytochromes acting as electron carriers need to accept electrons from an upstream donor. Commonly, this comes in the form of a quinol-cytochrome *c* oxidoreductase (QCR), which can contribute to the PMF *via* the Q-cycle. In order to investigate whether the QCR is involved in selenate respiration and could therefore be responsible for electron transfer to the di-heme cytochrome (cyt*c*-Ts4), classical inhibitors of respiratory chains were used during selenate and nitrite respiration. The inhibitors myxothiazol and antimycin A specifically inhibit the QCR, but at different sites (29). Myxothiazol binds to the Q_o site on the *b* heme subunit of QCR. The Q_o site is where quinol is oxidised to quinone, and the binding of myxothiazol stops electrons being transferred from the Q-pool to downstream electron acceptors. By contrast, antimycin A binds to the Q_i site of QCR preventing the reduction of quinone to quinol. HQNO (2-n-heptyl-4-hydroxyquinoline N-oxide) is a less specific quinone analogue which inhibits not only the QCR (30), but also the membrane bound nitrate reductase subunit NarI (31) and multi-heme quinol dehydrogenases such as NrfH from *Wolinella succinogenes* nitrite reductase (32).

In order to culture *T. selenatis* under more reproducible conditions, and allow multiple replicates of growth curves, a method of culturing *T. selenatis* in a 96 well microplate was devised. All growth conditions were replicated in 10 wells, allowing averaging of the optical densities over each time point. Before averaging, the optical density of a control set of wells of medium with no bacterial culture was subtracted from the growth curves. In order to test whether concentrations of inhibitor were high enough to inhibit *T. selenatis*, the microplate method was used to investigate the effect of myxothiazol on

nitrite respiration, to see if complete inhibition could be achieved. *Thauera* sp. is known to express a cd_1 nitrite reductase (33, 34) which commonly receives its electrons from the QCR via soluble intermediates (35). A range of nitrite concentrations were used, with myxothiazol at 10 μM. Ten wells contained 5 mM nitrite, but no inhibitor. Myxothiazol was seen to inhibit nitrite respiration very effectively and no growth was observed (Figure 6A). This confirms the effectiveness of myxothiazol as an inhibitor of the QCR in *T. selenatis*.

T. selenatis was cultured under selenate respiratory conditions, with varying concentrations of selenate and 10 μM myxothiazol. Ten wells contained 10 mM selenate but lacked myxothiazol, as a positive control. The resulting growth curves (Figure 6A) indicate that selenate respiration is partially inhibited by myxothiazol, suggesting that the QCR is involved in this process. The experiments were repeated in the presence of the inhibitor antimycin A (at both 10 μM and 20 μM) and the results (Figure 6B) are consistent with the observations made using myxothiazol, strongly indicating the involvement of QCR in electron transport. Again, even at 20 μM [antimycin], some growth is detected (final OD_{600nm} ~0.3 units). Analysis of the specific growth rates (μ_{max}) at increasing [selenate] shows that K_s is unaffected (~2.5 mM); however, in the presence of myxothiazol, a three-fold decrease in μ_{max} is recorded (No inhibitor = 0.32 ± 0.03 h^{-1}; plus myxothiazol = 0.10 ± 0.02 h^{-1}) (Figure 6C). Therefore, it can be seen, from the growth curve analysis, that both myxothiazol and antimycin A retard the growth rate of *T. selenatis* during selenate respiration, but does not inhibit it completely.

Inhibition of selenate respiration by HQNO - As myxothiazol has been shown to fully inhibit the QCR in nitrite reduction, but is only partially effective at inhibiting selenate respiration, HQNO was used as an inhibitor which affects a wider range of proteins with quinol dehydrogenase activity. HQNO was shown to inhibit growth completely with no significant change in culture OD for ~14 hours post inoculation. Cultures maintained for 14-18 hours showed a slight increase in culture OD presumably due to the break-down or evaporation of HQNO from the growth medium (Figure 6A). By combining both inhibitors, HQNO and myxothiazol, there was no significant difference between the growth curves obtained with HQNO alone. The results (Figure 6A) show that partial inhibition of selenate respiration is obtained by myxothiazol (and antimycin A) whereas complete inhibition of selenate respiration is obtained by HQNO. The combined data suggest that there is more than one route by which electrons can be transferred to selenate reductase; *via* the QCR which is inhibited by myxothiazol and antimycin A, and *via* another type of quinol dehydrogenase which is inhibited by HQNO.

DISCUSSION

The bioenergetics of selenate respiration in *T. selenatis* has remained unresolved since the isolation of *T. selenatis* by Macy and co-workers in 1993 (36). The respiration of selenate results in the sequential reduction of selenate to selenite to elemental selenium, yet it is only selenate that can function as a respiratory substrate. Selenate reductase (SER) is a soluble molybdoenzyme comprised of three subunits and is expressed from an operon of four genes (7), three for the structural components and the forth (SerD) a private chaperone for the functional assembly of SerA. No obvious membrane bound component has been identified. Whilst others have speculated as to how SER receives electrons from the Q-pool and how this is coupled to the generation of PMF (21), biochemical evidence for the electron transfer pathway in *T. selenatis* has remained wanting. In the present study we have demonstrated that SER can receive electrons from a di-heme cytochrome of the cytc_4 family and is driven by electron transfer *via* a branched pathway that includes electron transfer from QCR or QDH. The demonstration of an electron transfer pathway to a periplasmic molybdoezyme that utilises a high potential di-heme cytochrome *c* carrier and electron flux through QCR is the first of its kind and unprecedented in other molybdo-oxidoreductase systems.

A number of periplasmic *c*-type cytochromes were up-regulated when *T. selenatis* was grown on selenate as the sole electron acceptor. During this study, two of these cytochromes have been purified and tested as potential redox partners to SER. A 24k Da cytochrome, termed cyt*c*-Ts4 was shown to donate electrons to SER and was characterised further. N-terminal sequence and LC-MS/MS analysis identified peptides as those resulting from members of the cytochrome c_4 family. Attempts to PCR and sequence the cyt*c*-Ts4 gene using degenerate primers derived from other c_4 homologues failed. Consequently, a

holistic approach was adopted and the entire genome of *T. selenatis* was sequenced using an Illumina sequencer. The complete cyt*c*-Ts4 gene sequence was subsequently identified. A database search with the translated sequence of this gene produced a large number of similar proteins, most of which are classified as cytochromes c_4, a group of di-heme cytochromes *c* characterised by high redox potentials, a low intensity asymmetrical α band around 550 nm and a low α/β peak ratio (37,38). A number of members of this group have been characterised, including members from *Acidithiobacillus ferrooxidans* (39,40), *Pseudomonas stutzeri* (41), *Thiocapsa roseopersicina* (42) and *Azotobacter vinelandii* (43). Cytochromes c_4 have been proposed to be electron donors to oxidases due to the presence of a cytochrome c_4 in the aerobe *A. vinelandii* (43) but the discovery of a cytochrome c_4 in *T. roseopersicina*, a facultative anaerobic photosynthetic bacterium, suggests that their roles are much more varied (42,44). Recently, a cytc_4 has also been found to function as a physiological electron carrier in the photosynthetic electron transport chain in *Rubrivivax gelatinosus* (45).

Structural data is available for two cytochromes c_4, from *P. stutzeri* (46) and *A. ferrooxidans* (47). The two hemes in each case both have His-Met axial ligation, and the methionine residues identified as ligands are conserved throughout the cytochrome c_4 group, and in the cyt*c*-Ts4. The sequence similarity and high redox potential of the 24 kDa cytochrome suggest that we can assign cyt*c*-Ts4 to the cytochrome c_4 group. The involvement of a c_4 cytochrome in anaerobic selenate respiration defines a new role for this class of cytochromes.

Of the other cytochromes up-regulated during growth of *T. selenatis* on selenate, a 6kDa cytochrome was also purified (cyt*c*-Ts7). No evidence was obtained to suggest that cyt*c*-Ts7 could transfer electrons to SER. Furthermore, no direct reduction of selenate or selenite was observed. The function of cyt*c*-Ts7 remains to be established. Chlorate reductase from *I. dechloratans* is also a member of the TAT-translocated type II molybdo-enzymes and is closely related to SER. It has been shown recently that a 6 kDa cytochrome from *I. dechloratans* was readily oxidized in the presence of chlorate and cell homogenate containing chlorate reductase (Clr) (48), suggesting that a 6 kDa cytochrome could be the redox partner for Clr. The authors suggest that the 6 kDa cytochrome might accept electrons from QCR, but no biochemical evidence for the involvement of QCR was reported. More recently, a cytochrome *c* gene located at the gene cluster for chlorate respiration in *I. dechloratans* has been cloned and over-expressed in *E. coli* but demonstrated not to function as an electron donor to purified chlorate reductase (49). It is interesting to speculate what the functions of the additional *c*-type cytochromes are in *T. selenatis* when grown on selenate. The mechanism by which selenite is reduced remains unknown. What is clear is that the reduction of selenite results in the formation of selenium nanospheres that are found in the surrounding medium. For the elemental selenium to form extra-cellular particles it is considered likely that selenite is reduced either in the periplasm or on the outer cell surface, and as a consequence the other cytochromes identified might form an electron conduit to selenite reductase.

The involvement of QCR in the respiratory electron transfer chain of *T. selenatis* was suggested from the genome analysis (*Genbank accession* EU732596.1) and confirmed by complete inhibition of nitrite respiration by myxothiazol. *T. selenatis* expresses a cd_1 nitrite reductase (also identified in the *T. selenatis* genome (*Genbank accession* AY078264.1) which commonly receives electrons from QCR *via* soluble intermediates (cytochromes/azurins). Selenate respiration was only partially inhibited (70% reduction in μ_{max}) by the same concentration of myxothiazol or antimycin A and completely inhibited by HQNO. QCR binds two quinol molecules at the periplasmic face of the membrane and moves two electrons to the cytoplasmic face of the membrane, where it reduces one quinone molecule. This so called Q-cycle translocates two positive charges per quinol oxidized. Given that myxothiazol and antimycin A are specific inhibitors of QCR, a redox loop coupling a Q-cycle mechanism to selenate reduction would seem plausible. HQNO is a less specific quinone analogue which inhibits both QCR and other membrane-bound QDHs (31,32). HQNO alone, or in combination with myxothiazol, resulted in the complete inhibition of growth of *T. selenatis*. These data suggest that selenate reductase can accept electrons from more that one electron donor. A branched pathway that involves both QCR and QDH is proposed (Figure 7). A QDH partner has not been identified, but analysis of the *c*-type cytochromes in membrane fractions from *T. selenatis,* grown on selenate, reveals that cytochromes of ~30 kDa and ~20 kDa are present, but attempts to purify these

components have so far proved unsuccessful (data not shown). A *nap*C/*nir*T homologue (50) has also been identified in the *T. selenatis* genome that could be a likely candidate.

The ability to utilise a QCR dependent bioenergetic pathway is facilitated by the high redox potential of the selenate/selenite couple (E_m +475 mV). This allows the selenate reductase to function by using a high potential cytochrome *c* as the electron donor. The interesting feature of SER thus relates to the point of electron entry and the unusual *b*-heme in SerC. The determination of the redox potential of the SerC heme has allowed us to add to our knowledge of the redox centres of the selenate reductase and is the first periplasmic reductase of the Type II molybdo-enzymes to have the potential of its *b*-heme determined. Figure S2 (supplemental) shows the known midpoint potentials of all redox centres within SER, from the redox potential of the substrate to the potential of *b*-heme subunit. The value of E_m = +234 ±10 mV for the SerC *b*-heme is very similar to that determined for EbdC (+254 mV). EBDH functions by withdrawing electrons from ethylbenzene, where the *b*-heme functions as an electron attractant. Conceptually, to convert from a dehydrogenase function to a reductase function, one might assume that the potential of the corresponding *b*-heme in the type II molybdo-reductases might be retuned to function at a much lower redox-potential, thus facilitating electron donation. This appears not to be the case for selenate reductase. It is of interest to compare SerC/EbdC cytochromes to the membrane-bound cytochrome associated with the respiratory nitrate reductase (NarI). NarI contains two *b*-hemes, but both have much lower redox potential (+120 and +20 mV). Modelling the three dimensional structure of SerC, using the X-ray co-ordinates of EbdC from *A. aromaticum*, predicts that the *b*-heme in SerC is also co-ordinated by methionine (M138) and lysine (K228) ligands (Figure 8). In NarI, both hemes have Fe with *bis*-histidinyl co-ordination and this could contribute to the differences in redox potential. The sulfur of methionine residues is a good electron acceptor, and could contribute to stabilizing the reduced state of the heme, therefore significantly raising the midpoint potential.

Evidently the combination of a high potential *b*-heme in SerC and the unusual high potential redox couple of the substrate (selenate/selenite) has provided a system that can readily accept electrons from cyt-*c* and QCR redox partners. By using these redox partners, selenate reduction can be linked to a Q-cycle mechanism. Since selenate reductase functions on the positive side of the cytoplasmic membrane, the reduction of selenate to selenite will consume two pumped protons. If SER was to receive electrons only from a membrane-bound quinol dehydrogenase (QDH), then only two protons would be released to the periplasm, resulting in no net gain of proton electro-chemical gradient ($0q^+/2e^-$). Because the reduction of selenite to selenium does not support growth, selenate reduction *via* a QDH could only be energy conserving if electron input into the Q-pool was proton-motive (i.e. *via* an NADH dehydrogenase, a formate dydrogenase, or hydrogenase). By using the Q-cycle mechanism a net gain of $2q^+/2e^-$ of proton electrochemical gradient can be maintained irrespective of the electron donor.

Finally, the Q-cycle coupling mechanism presented for selenate reduction in *T. selenatis*, whilst a novel mechanism for electron transport to molybdoezymes in bacteria, might also be utilised in the Archaea (51). Sequence analysis has suggested that the clade of TAT-translocated type II molybdoenzymes, of which SER is a member, also contains a number of unusual respiratory nitrate reductases (pNAR). These reductases all possess a TAT leader peptide and are translocated to the positive side of the membrane. The pNAR enzymes are distributed amongst the Archaea and examples have been identified in the hythermophiles and halophiles. Interestingly, those from halophiles (*Haloferax mediterranei* and *Haloarcula marismortui*), lack a NarI-like component so the mechanism of electron transport is not obvious. However, genetic analysis reveals the presence of a sequence that encodes a protein (NarC) similar to the di-heme subunits of QCR. Adjacent to the *nar*C gene is a gene that encodes NarB which is predicted to encode a Rieske iron-sulfur protein. The combination of NarB and NarC in *H. mediterranei* has led to the suggestion that nitrate respiration in some organisms might be driven by a Q-cycle mechanism (51). By coupling a Q-cycle mechanism to nitrate reduction would provide a pNAR system that is bioenergetically equivalent to the well characterised NAR (or nNAR) systems in bacteria.

ACKNOWLEDGMENTS

We thank Ann Reilly (University of East Anglia), Iona Knight (University of Exeter), Dr Carys Watts and Dr Helen Ridley (University of

Newcastle) for technical support and useful discussions. We also thank Dr Kirsty Line (University of Exeter) for providing structural models.

REFERENCES

1. McDevitt, C.A., Hugenholtz, P., Hanson, G.R. and McEwan, A.G. (2002) *Mol. Microbiol.* **44**, 1575-1587
2. Berks, B.C., Sargent, F. and Palmer, T. (2000) *Mol. Microbiol.* **35**, 260-274
3. Sargent, F. (2007) *Microbiology* SGM **153**, 633-651
4. Johnson, H.A., Pelletier, D.A. and Spormann, A.M. (2001) *J. Bacteriol.* **183,** 4536-4542
5. McDevitt, C.A., Hanson, G.R., Noble, C.J., Cheesman, M.R. and McEwan, A.G. (2002) *Biochemistry* **41**, 15234-15244
6. Schröder, I., Rech, S., Krafft, T. and Macy, J.M. (1997) *J. Biol. Chem.* **272,** 23765-23768
7. Krafft, T., Bowen, A., Theis, F. and Macy, J.M. (2000) *DNA Seq.* **10**, 365-377
8. Thorell, H.D., Stenklo, K., Karlsson, J. and Nilsson, T. (2003) *Appl. Environ. Microbiol.* **69**, 5585-5592
9. Karlsson, J. and Nilsson, T. (2005) *Protein Expr. Purif.* **41**, 306-312
10. Creevey, N.L., McEwan, A.G., Hanson, G.R. and Bernhardt, P.V. (2008) *Biochemistry* **47**, 3770-3776
11. Dridge, E.J., Watts, C.A., Jepson, B.J.N., Line, K., Santini, J.M., Richardson, D.J. and Butler, C.S. (2007) *Biochem. J.* **408**, 19-28
12. Richardson, D. J. (2000) *Microbiology* **146**, 551-571
13. Stolz, J.F., Basu, P., Santini, J.M. and Oremland, R.S. (2006) *Annu. Rev. Microbiol.* **60**, 107-130
14. Maher, M.J., Santini, J., Pickering, I.J., Prince, R.C., Macy, J.M. and George, G.N. (2004) *Inorg. Chem.* **43,** 402-404
15. Kloer, D.P., Hagel, C., Heider, J. and Schulz, G.E. (2006) *Structure* **14**, 1377-1388
16. Bertero, M.G., Rothery, R.A., Palak, M., Hou, C., Lim, D., Blasco, F., Weiner, J.H. and Strynadka, N.C. (2003) *Nat. Struct. Biol.* **10**, 681-687
17. McCrindle, S. L., Kappler, U. and McEwan, A. G. (2005) *Adv. Microb. Physiol.* **50**, 147-198
18. Jormakka, M., Richardson, D.J., Byrne, B. and Iwata, S. (2004) *Structure* **12**, 95-104
19. Potter, L., Angove, H., Richardson, D. and Cole, J. (2001) *Adv. Microb. Physiol.* **45**, 51-112
20. Brondijk, T. H., Nilavongse, A., Filenko, N., Richardson, D. J. and Cole, J. A. (2004) *Biochem. J.* **379**, 47-55
21. McEwan, A. G., Ridge, J. P., McDevitt, C. A. and Hugenholtz, P. (2002) *Geomicrobiology Journal* **19**, 3-21
22. Ridley, H., Watts, C.A., Richardson, D.J. and Butler, C.S. (2006) *Appl. Environ. Micro.* **72**, 5173-5180
23. Dutton, P.L. (1978) In *Methods in enzymology; Biomembranes E, specialized techniques*. Vol. 54. Fleischer, S. and Packer, L. (eds). New York ; London: Academic Press, pp. 411-435
24. Zerbino, D.R. and Birney E. (2008) *Genome Research* **18**, 821-829
25. Zwietering, M.H., Rombouts, F.M and Van't Riet, K. (1992) *J. Appl. Bacteriol.* **72**, 139-145
26. Monod, J. (1942) *Recherches sur la croissance des cultures bactâeriennes,* p. 211. Hermann, Paris.
27. Craske, A.L and Ferguson, S.J. (1986) *Eur. J. Biochem.* **158**, 429-436
28. Altschul, S.F., Gish, W., Miller, W., Myers, E.W. and Lipman, D.J. (1990) *J. Mol. Biol.* **215**, 403-410
29. Thierbach, G. and Reichenbach, H. (1981) *Biochim. Biophys. Acta* **638**, 282-289
30. Van Ark, G. and Berden, J. A., (1977) *Biochim. Biophys. Acta* **459**, 119-127
31. Magalon, A., Rothery, R. A., Lemesle-Meunier, D., Frixon, C., Weiner, J. H. and Blasco, F. (1998) *J. Biol. Chem.* **273**, 10851-10856
32. Simon, J. (2002) *FEMS Microbiol. Rev.* **26**, 285-309
33. Etchebehere, C. and Tiedje, J. (2005) *Appl. Environ. Microbiol.* **71**, 5642-5645
34. Song, B. and Ward, B.B. (2003) FEMS *Microbiol. Ecol.* **43**, 349-357
35. Moir, J. W., Baratta, D., Richardson, D. J. and Ferguson, S. J., (1993) *Eur. J. Biochem.* **212**, 377-385
36. Macy, J.M., Rech, S., Auling, G., Dorsch, M., Stackenbrandt, E. and Sly, L.I. (1993) *Int. J. Syst. Bacteriol.* **43,** 135-142
37. Pettigrew, G.W. and Moore, G.R. (1987) *Cytochromes c : biological aspects.* Berlin: Springer.
38. Pettigrew, G.W. and Brown, K.R. (1988) *Biochem. J.* **252**, 427-435

39. Cavazza, C., Giudici-Orticoni, M.T., Nitschke, W., Appia, C., Bonnefoy, V. and Bruschi, M. (1996) *Eur. J. Biochem.* **242**, 308-314
40. Giudici-Orticoni, M.T., Leroy, G., Nitschke, W. and Bruschi, M. (2000) *Biochemistry* **39**, 7205-7211
41. Christensen, H.E. (1994) *Gene* **144**, 139-140
42. Branca, R.M., Bodo, G., Varkonyi, Z., Debreczeny, M., Osz, J. and Bagyinka, C. (2007b) *Arch. Biochem. Biophys.* **467**, 174-184
43. Swank, R.T. and Burris, R.H. (1969) *Biochim Biophys Acta* **180**, 473-489
44. Branca, R.M., Bodo, G., Bagyinka, C. and Prokai, L. (2007a) *J. Mass. Spectrom.* **42**, 1569-1582
45. Ohmine, M., Matsuura, K., Shimada, K., Alric, J., Verméglio, A. and Nagashima, K.V. (2009) *Biochemistry* **48**, 9132-9139
46. Kadziola, A. and Larsen, S. (1997) *Structure* **5**, 203-216
47. Abergel, C., Nitschke, W., Malarte, G., Bruschi, M., Claverie, J.M. and Giudici-Orticoni, M.T. (2003) *Structure* **11**, 547-555
48. Bäcklund, A.S., Bohlin, J., Gustavsson, N. and Nilsson, T. (2009) *Appl. Environ. Microbiol.* **75**, 2439 -2445
49. Bohlin, J., Bäcklund, A.S., Gustavsson, N., Wahlberg, S. and Nilsson, T. (2009) Microbiol. Res. Dec 14. [Epub ahead of print] doi:10.1016/j.micres.2009.10.003
50. Roldan, M. D., Sears, H. J., Cheesman, M. R., Ferguson, S. J., Thomson, A. J., Berks, B. C. and Richardson, D. J. (1998) *J. Biol. Chem.* **273**, 28785-28790
51. Martinez-Espinosa, R. M., Dridge, E. J., Bonete, M. J., Butt, J. N., Butler, C. S., Sargent, F. and Richardson, D. J. (2007) *FEMS Microbiol. Lett.* **276**, 129-139
52. Morris, A.L., MacArthur, M.W., Hutchinson, E.G. and Thornton, J.M. (1992) *Proteins* **12**, 345-364
53. Laskowski, R.A., MacArthur, M.W., Moss, D.S. and Thornton, J.M. (1993). *J. Appl. Cryst.* **26**, 283-291
54. DeLano, W.L. (2002) The PyMOL Molecular Graphics System, DeLano Scientific, San Carlos, CA, USA. http://www.pymol.org.

FOOTNOTES

*This work was funded in part by research grants from the BBSRC (P17219 and BBS/B/10110) to CSB and DJR, and BBSRC/EPSRC (life science interface) grant (BB/D00781X/1) to CSB, RJL and DJR. ECL was a recipient of a BBSRC Agri-food committee studentship. SB was supported by a La Trobe University postgraduate award. Sequencing of the *T. selenatis* genome was funded by the Systems Biology Theme, University of Exeter.

FIGURE LEGENDS

Figure 1. Subunit organisation and redox cofactors of periplasmic type II molybdoenzymes. Direction of electron transfer is indicated by the arrows. Reductases include selenate and chlorate reductase. Dehydrogenases include dimethylsulphide and ethylbenzene dehydrogenases.

Figure 2. Cytochrome *c* profile from *T. selenatis*. A; SDS-PAGE gels stained for *c*-type cytochromes, showing periplasmic cytochromes (cyt*c*-Ts1-7) expressed during selenate and/or nitrate respiration. Lane 1 – Invitrogen SeeBlue Plus2 Prestained Standard. Lane 2 – periplasmic fraction from selenate grown cells (heme stained). Lane 3 – periplasmic fraction from nitrate grown cells (heme stained). 7 μg of protein was loaded in each lane. Lane 4; purified cyt*c*-Ts4 (~24 kDa) stained with Invitrogen SeeBlue Plus2. Lane 5 purified cyt*c*-Ts4 (~24 kDa) stained with heme stain. Lane 6 purified cyt*c*-Ts7 (~6 kDa) stained with Invitrogen SeeBlue Plus2. Lane 7 purified cyt*c*-Ts7 (~6 kDa) stained with heme stain. **B;** Spectra of 25 μM cyt*c*-Ts4 (~24 kDa protein) as purified (solid line), reduced with sodium dithionite (dotted line) and oxidized with potassium ferricyanide (dashed line). **C;** Spectra of 25 μM cyt*c*-Ts7 (~6 kDa protetin) as purified (solid line), reduced with sodium dithionite (dotted line) and oxidized with potassium ferricyanide (dashed line).

Figure 3. Spectroscopic assay of electron donation from cyt*c*-Ts4 to SerABC. Cyt*c*-Ts4 (5 μM) reduced with dithionite (dashed line) was mixed with 1 μM SerABC and 20 mM selenate and re-oxidation was monitored by wavelength scanning UV-visible spectroscopy (solid line).

Figure 4. Optical redox titration of cyt*c*-Ts4. A; α and β region of cyt*c*-Ts4 spectrum during titrations. Black arrow indicates increasing redox potential. **B;** Fraction of cytochrome reduced as calculated with reference to absorbance at 551 nm, as a function of redox potential. Nernst curves for n=1 electrons (dashed line) and n=2 electrons (solid line) are also shown.

Figure 5. Optical redox titration of SerC. A; shows the α and β region of *b*-heme spectrum during titrations. Black arrow indicates increasing redox potential. Samples were prepared in 30 mM Tris-HCl pH7.5. **B**; Fraction of cytochrome *b* reduced as calculated with reference to absorbance at 558 nm, as a function of redox potential. Nernst curve for n=1 electron.

Figure 6. Inhibition of respiration by myxothiazol, antimycin A and HQNO. A; Optical density of *T. selenatis* cultures grown with 10 mM selenate as electron acceptor in the absence and presence of inhibitors. No inhibitor (■); 10 μM myxothiazol (◆); 20 μM HQNO (●) and both 10 μM myxothiazol and 20μM HQNO (▼). Positive control: *T. selenatis* grown with 5 mM nitrite as electron acceptor in the presence of 10 μM myxothiazol (○). B; Optical density of *T. selenatis* cultures grown with 10 mM selenate as electron acceptor in the absence and presence of antimycin A. No inhibitor (■); 10 μM antimycin A (◆); 20 μM antimycin A (●). C; Specific growth rate (μ_{max}) of *T. selenatis* cultures grown on increasing [selenate] in the absence (■) and presence of myxothiazol (●) (10 μM). In all cases error bars represent standard deviation of n=10 cultures.

Figure 7. Schematic diagram showing the electron transport chain of *T. selenatis* during anaerobic growth on selenate.

Figure 8. *b*-heme co-ordination in SerC. A: Predicted structure of SerC modelled upon the crystal structure of EBDH γ-subunit. Superposition shown; SerC is in green and the EbdC is in cyan. **B**: Detail of heme pocket showing ligands. Homology modelling was performed using the homology tools in the software package MOE™. The sequence of *T. selenatis* SerC was aligned and modelled against the structure of EBDH γ-subunit from *A. aromaticum* (PDB – 2IVF C). The sequence was modelled from residues 27 to 239. The modelling was performed using the protein template alone, and additionally using the environment of the template structure with the heme ligand. An ensemble of 30 intermediate models was created and the best intermediate model as minimized using the CHARM22 force field to an RMS gradient of 0.01. The quality of the models was assessed by PROCHECK (52, 53). Analysis of the model structure and generation of molecular images were carried out using PyMol (54).

Lowe *et al*. **Figure 1**

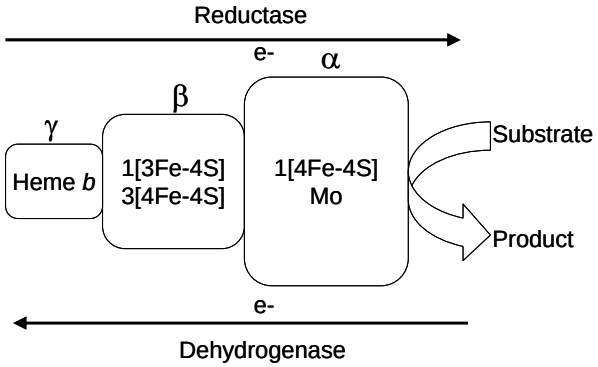

Lowe *et al*. **Figure 2**

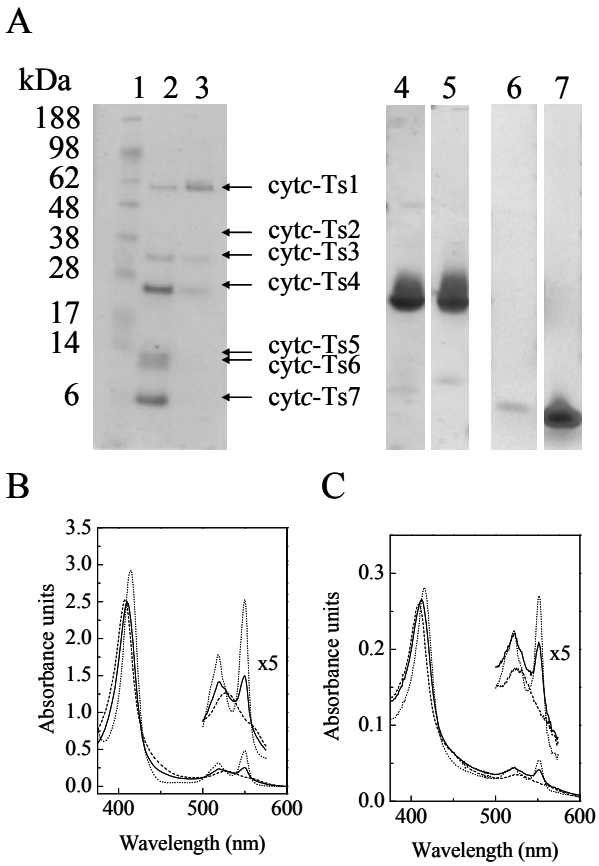

Lowe *et al*. **Figure 3**

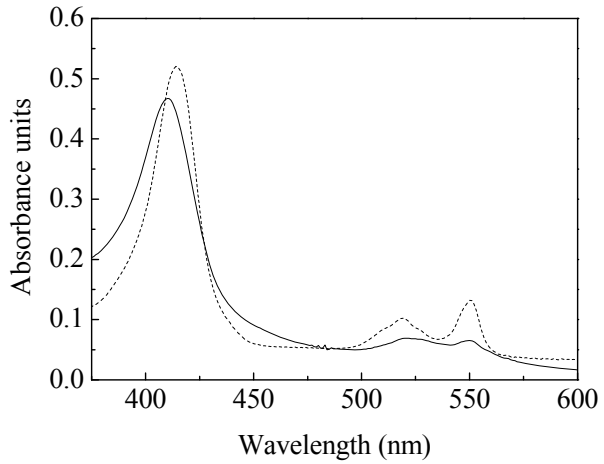

Lowe *et al*. **Figure 4**

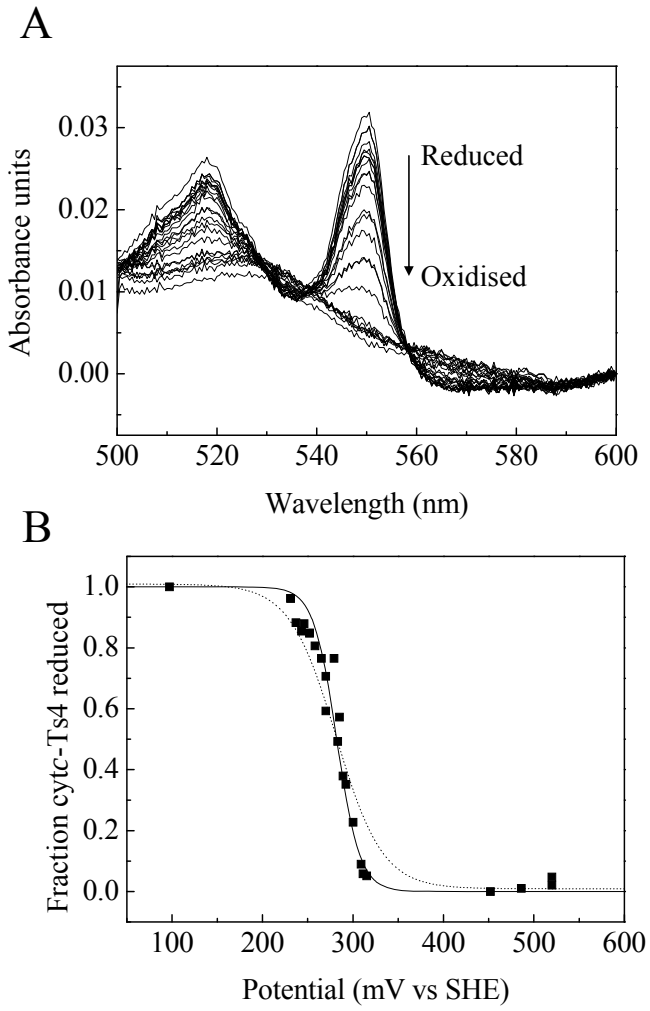

Lowe *et al*. **Figure 5**

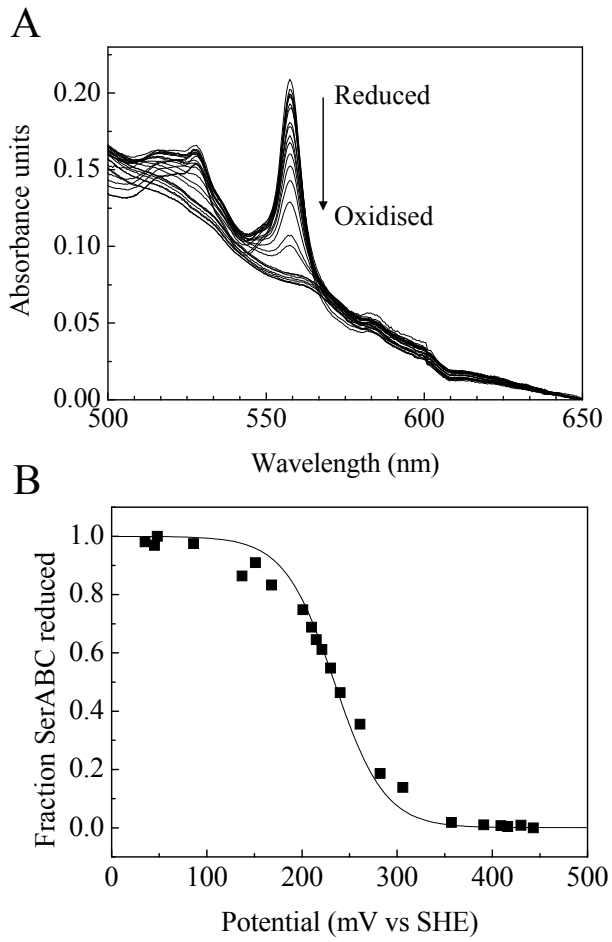

Lowe *et al.* **Figure 6**

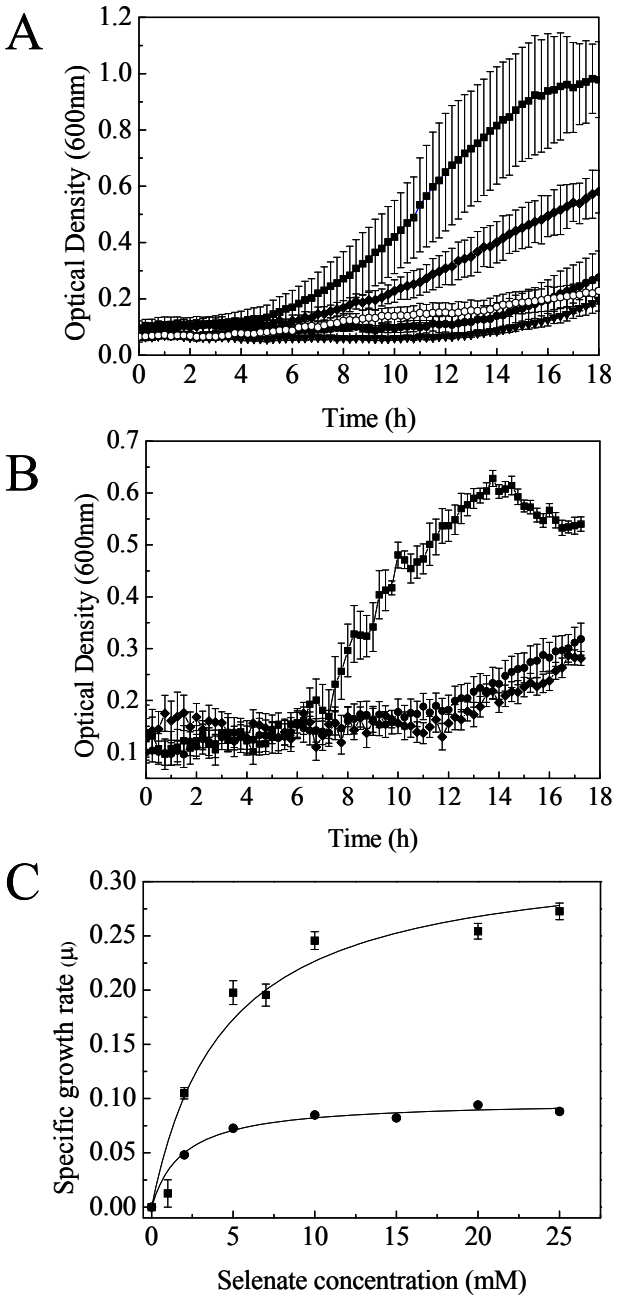

Lowe *et al.* **Figure 7**

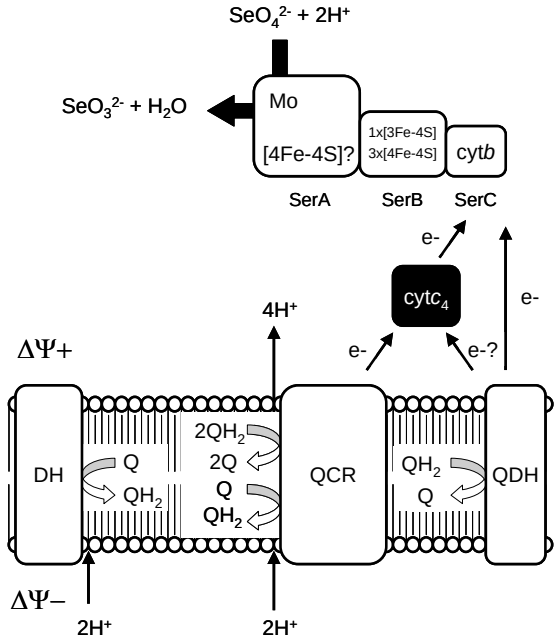

Lowe *et al*. **Figure 8**

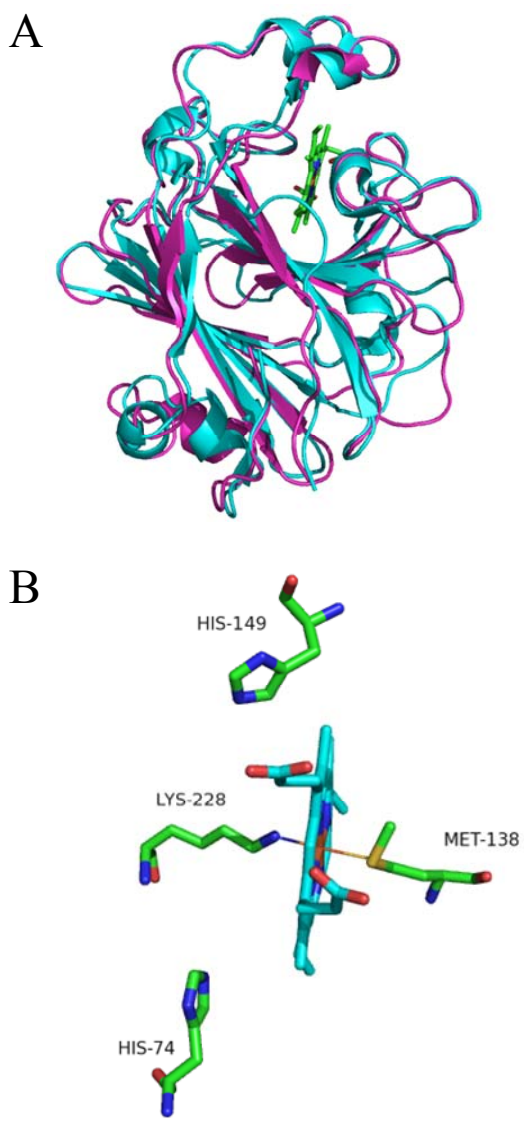

Supplementary material - Lowe *et al*.

Figure S1. Sequence alignments of cytochromes c_4 and sequence for the 24 kDa cytochrome *c* from *T. selenatis*. Bacterial strains from which sequence data is taken are abbreviated as follows (Genbank accession numbers for protein sequences are in parenthesis); Ts – *Thauera selenatis* (GU570563), Da – *Dechlomonas aromatica* RCB (AAZ46318.1), Mg – *Magnetospirillum gryphiswaldense* MSR1 (CAM74905.1). Mm – *Magnetospirillum magneticum* (BAE51887.1), Ps – *Pseudomonas stutzeri* (AAA20247.1|), Af – *Acidithiobacillus ferrooxidans* (CAA07032.1), Pp – *Pseudomonas putida* GB-1 (ABY96057.1), Av – *Azotobacter vinelandii* (AAA87314.1), Sb – *Shewanella baltica* OS195 (ABN59587.1), So – *Shewanella oneidensis* MR-1 (AE015898_8), Vp – *Vibrio parahemeolyticus* AQ3810 (EDM58639.1), Pe – *Pseudomonas entomophila* L48 (CAK13073.1) and Tr – *Thiocapsa roseopersicina* (P86052.1). Cytochrome *c* binding motifs (CXXCH) and conserved axial methionine residues (M) are underlined. All conserved residues are marked with an asterisk.

Figure S2. Electron transfer during selenate respiration. The known E_m values of each of the components involved in electron transfer to selenate through the selenate reductase system. Q-pool indicates ubiquinol (Eo'~+65 mV) and menaquinol (Eo'~-55 mV). Arrows indicate direction of electron transfer.

Lowe *et al*. **Figure S1**

```
Ts    ------------GPPAPKK-EGIEGQGYVWNAQEGEKIEALQKKGDVTRGEEAYEVCGACHLPSG
Da    ------------GPPAPHK-EGIESKDYKWNAEGGEKMEALHKKGNVKNGEEVYEICGACHLPSG
Mg    -------------KDKPAQGKLLGDKDYQWNANGGEKDEAEHLKPDLKNGRDVYEVCAACHLPEG
Mm    ----------AGGG-TPQKGKSLGEEGYQWHAGGGEEDEALHLKPDLANGKEVYEVCSACHQMEG
Ps    --------------------------------AGDAEAGQGKV-----------AVCGACHGVDG
Af    -------------------------------AVGSADAPAPYRVS----------SDCMVCHGMTG
Pp    --------------------------AQPIKGDAAAGQAKT-----------AVCGACHNPDG
Av    -------------------------------AGDAAAGQGKA-----------AVCGACHGPDG
Sb    -------------------------------EGNAEAGKTKI-----------IVCSACHGMDG
So    -------------------------------EGNAEAGKTKI-----------IVCSACHGMDG
Tr    --------------------TDGHQAAAPQVGDPQAGEAKAN----------GVCLACHGPQG
                                                           *  **   *

Ts    AGRPDGTFPQLAGQHTTVLIKQMADIRAGL---------RDNPTMYPFAA--TLVDPQELADVSA
Da    AGRADGTFPQLAGQHSTVLIKQMADIRSGE---------RDNPTMYPFAS--TLTDPQELADAAA
Mg    WGQTDGTFPQLAGQHPKVIIKQLADIRALN---------RDNPTMYPFALPDQIGGPQAIADVAA
Mn    WGLTDGTFPQLAGQHPKVVIKQLADIRALN---------RDNPTMYPFALPSQIGGPQAIADVAA
Ps    -NSPAPNFPKLAGQGERYLLKQLQDIKAGSTPGAPEGVGRKVLEMTGMLDP---LSDQDLEDIAA
Af    RDTLYPIVPRLAGQHKSYMEAQLKAYKDHSRADQ-----NGEIYMWPVAQA---LDSAKITALAD
Pp    -NSLAPNFPKLAGQGQRYLEKQLHDIKSGK---------RTVLEMTGMLTA---FSDQDLADIAA
Av    -NSAAPNFPKLAGQGERYLLKQMQDIKAGTKPGAPEGSGRKVLEMTGMLDN---FSDQDLADLAA
Sb    -NSMIDMYPKLAGQHATYLQKQLHDFRSAAQTGGKDG--RMDPIMSGMAMP---LSDQDILDITA
So    -NSMIDMYPKLAGQHATYLQKQIHDFRSAAQSGGKDG--RMDPIMSGMAMP---LSDQDILDISA
Tr    -NSLVPIWPKLAGQHPEYIVKQLMDFKQRR----------ANEQMTPMAMP---LTDQEVLDLAA
             * ****       *                      *

Ts    YIESLCIPTDHGKYEGADA--ALQVAKGKELYE--KQCKECHGDTG-AGDKAKFYPVIAGQHYKY
Da    YINSLCIPLEHGKYEGADA--AMQIAKGKELYE--KECLECHGKTG-EGNKEKFYPVIAGQHYKY
Mg    YIQ----KLKMNPEPGVGD--GKDLEHGKKLYK--DNCVRCHGEHG-EGNNDKYYPRLEGQHYNY
Mn    YMAV---KLKMNPEPGVGD--GKDLAHGKKLYE--ENCTRCHGADG-AGDNDKFYPRIQGQHYEY
Ps    YFSSQKGSVGYADPALAKQ--GEKLFRGGKLDQGMPACTGCHAPNG-VGNDLAGFPKLGGQHAAY
Af    YFNAQKPPMQSSGIKHAGAKEGKAIFNQGVTNEQIPACMECHGSDG-QGAG--PFPRLAGQRYGY
Pp    YFSSQKGSVGAADPKLVER--GRSLFNGGDLEKGMPACTGCHSPNG-AGIALAGFPHLGGQHSQY
Av    YFTSQKPTVGAADPQLVEA--GETLYRGGKLADGMPACTGCHSPNG-EGNTPAAYPRLSGQHAQY
Sb    YFSSQ-AIQVAEAKDVPEL--GAKLYKGGDVSRGITACMACHGPDG-KGAELAGFPTLAGQHANY
So    YFSTQ-KIQVAEVKDVPEL--GAKLYKGGDVSRGITACMACHGPDG-KGAESAGFPALAGQHANY
Tr    YYATQPKTPGAADPELASK--GESLYRWGNPETGVPACSGCHGPAGGAGQSLAKFPRLSAQHADY
      *                                  *  **   *  *      *    *   *

Ts    LLRQMTEIR--DGHRRNANP--DMVKVIKPYTDDQLVAISAYQASLKMPGSMC----GDKK----
Da    LLRQMTEIR--DGKRRNANP--DMVKIIKKYDNQQLIAISAYQSSMVMPGAMCKPKAGKKK----
Mg    LIRQYQWIK--EGKRRNANP--DMVQQIKTFTDRDTKAVLDYVSRIKPPANLIGTKGWQNPDFQ-
Mn    LLRQYQWIK--EGKRRNANP--DMMKQIQSFTDRDTKAVLDYTSRLKPPANLVAPKGWKNPDFQ-
Ps    TAKQLTDFR--EGNRTNDGDTMIMRGVAAKLSNKDIEALSSYIQGLH-----------------
Af    IIQQLTYFH--NGTRVN----TLMNQIAKNITVAQMKDVAAYLLSS-----------------
Pp    VTKQLTDFR--EGNRTNDGDAMTMRTIAGKLSNHDIEALASYIQGLH-----------------
Av    VAKQLTDFR--EGARTNDGDNMIMRSIAAKLSNKDIAAISSYIQGLH-----------------
Sb    IKIQLTKFR--EAGRHNDLN-GMMQDVAKKLSDSDIDALSKYLSSLK-----------------
So    IKLQLTKFR--DAGRHNDLN-GMMQDVAKKLNDSDIDALSKYLASLK-----------------
Tr    TKQTLEHFR--GALRANDPNG-MMRGAAARLSDQEIAAVSQYLQGLSQ-----------------
                    * *      *                   *
```

Lowe *et al*. **Figure S2**